Electronic Supplementary Material (ESI) for Sustainable Energy & Fuels.

Supporting Information

Electrochemical Deposition of Electronic Rich Pt Single Atoms and Nanocrystals on Porous Carbon for Enhanced Electrocatalysis in Strong Acid

Fang Cheng,[a] Shuai Yang,[d] Zongtao Zhao,[b] Chao Lin,[b] Haojie Zhang,[b] Xiaokai Song,*[a] Yong Qin[b] and Xiaopeng Li*[b]

*To whom correspondence should be addressed.

E-mail: xksong@jsut.edu.cn (X. S.); xiaopeng.li@dhu.edu.cn (X. L.)

Experimental Section

Chemicals and materials

2-methylimidazole (98%) and Nafion (5 wt.%) were purchased from Energy Chemical Co., Ltd. and Sigma-Aldrich, respectively. Other reagents and solvents were purchased from Sinopharm Co. Ltd. and used without further purification. Deionized (DI) water with resistivity higher than 18 MΩ cm was used during the experiments.

Preparation of Pt/CoNP/CoN$_x$/CNB and Pt/CNB

Core-shell structural ZnO@Zn/Co-ZIF composites were prepared by a typical solvothermal reaction using ZnO nanosphere (ZnONS) templates with an average diameter of ca. ~400 nm. The ZnO@Zn/Co-ZIF composites were then pyrolyzed at 900 °C in a tube furnace with a heating rate of 5 °C min^{-1} under flowing N_2 (50 cc min^{-1}) atmosphere to yield CoNP/CoN$_x$/CNB. For preparation of CNB, a same procedure was used, except for the addition of cobalt nitrate during the preparation of ZnO@ZIF precursor.

Pt/CoNP/CoN$_x$/CNB was synthesized by an electrochemical cycling approach, which was performed using a PARSTAT 4000 electrochemical workstation (Princeton Applied Research) and a standard three-electrode cell containing N_2-saturated 0.5 M H_2SO_4 at room temperature. CoNP/CoN$_x$/CNB was used as working electrode (the electrode preparation details seeing electrochemical measurements section), and a Pt wire and Ag/AgCl (Metrohm, saturated KCl) served as counter and reference electrodes, respectively. Constant electrochemical cycling of 6000 cycles in the potential range from 0.71 V to -0.39 V was conducted to prepare Pt/CoNP/CoN$_x$/CNB. Pt//CNB was synthesized using a same cycling approach when CNB was used as the working electrode.

Characterization

The morphology of the samples was characterized by field-emission SEM (Carl Zeiss Microscopy GmbH Supra 55) and TEM (FEI Tecnai G2). The high-angle annular dark-field scanning transmission electron microscopy (HAADF-STEM) images were performed on a JEOL JEM-2100F fieldemission transmission electron microscope. The atomic-resolution spherical aberration corrected Scanning Transmission Electron Microscope (AC-STEM) characterization was performed using a probe aberration-corrected microscope, JEMARM200F equipped with cold emitter, operated at 200kV. The attainable spatial resolution of this microscope is 78 pm. Powder X-ray diffraction (PXRD) patterns were recorded in a PANalytical diffractometer Model PW3040/60 X'pert PRO using monochromated Cu Kα radiation (40 kV, 40 mA) at a scanning rate of $2°\cdot\text{min}^{-1}$. Nitrogen sorption measurement was conducted using a Micromeritics ASAP 2020 system at 77 K. The X-ray photoelectron spectroscopy (XPS) was performed using the Thermo Scientific K-Alpha X-ray photoelelectron spectrometer with Al Kα X-ray source. Binding energy was calibrated by setting binding energy of C1s peak to 284.8 eV. The Pt content in the catalyst was conducted on the coupled plasma optical emission spectrometry (ICP-OES).

Electrochemical measurements

All electrochemical measurements were performed using PARSTAT 4000 electrochemical workstation (Princeton Applied Research) at room temperature. A Pt wire and Ag/AgCl (Metrohm, saturated KCl) served as counter and reference electrodes, respectively. The ORR electrocatalytic activity was measured by a rotating disk electrode (PINE, 5 mm diameter, 0.196 cm^2) technique. The glassy carbon electrode was polished to a mirror finish and thoroughly cleaned prior to use. To prepare the working electrode, 5 mg of the catalyst was dispersed in water and ethanol mixed solvent (1 mL, v/v = 3:1) with 40 μL of 5 wt % Nafion solution. Then the mixture was ultrasonicated for 60 min to generate a homogeneous ink. Next, 8 μL of dispersion was drop-casted onto the glassy carbon surface with a 0.2 mg cm^{-2} loading for all samples. Finally, the as-prepared catalyst film was dried at room temperature.

After 6000 constant potential cycles, the Pt/CoNP/CoN_x/CNB electrode was directly used for ORR performance tests. 0.5 M H_2SO_4 solution was used as the electrolyte at room temperature and purged with a high-purity O_2 flow for at least 30 min prior to the measurements. The linear scan voltammograms (LSV) were measured at a scanning rate 50 mV s^{-1} from 0.197 to 1.159 V vs. RHE at the rotating speed of 1600 using a Pt wire and Ag/AgCl (Metrohm, saturated KCl) as counter and reference electrodes, respectively. Chronoamperometric responses were recorded at 0.367 V vs. RHE using a graphite and Ag/AgCl (Metrohm, saturated KCl) as counter and reference electrodes, respectively. For comparison, Pt/CNB, CoNP/CoN_x/CNB, CNB, and Pt/C (20 wt% platinum, JM) was conducted on the same electrochemical tests. The electrode potential is reported against the reversible hydrogen electrode (RHE), calculated from the equation: E(RHE)= E(Ag/AgCl)+ 0.197+0.0591pH.

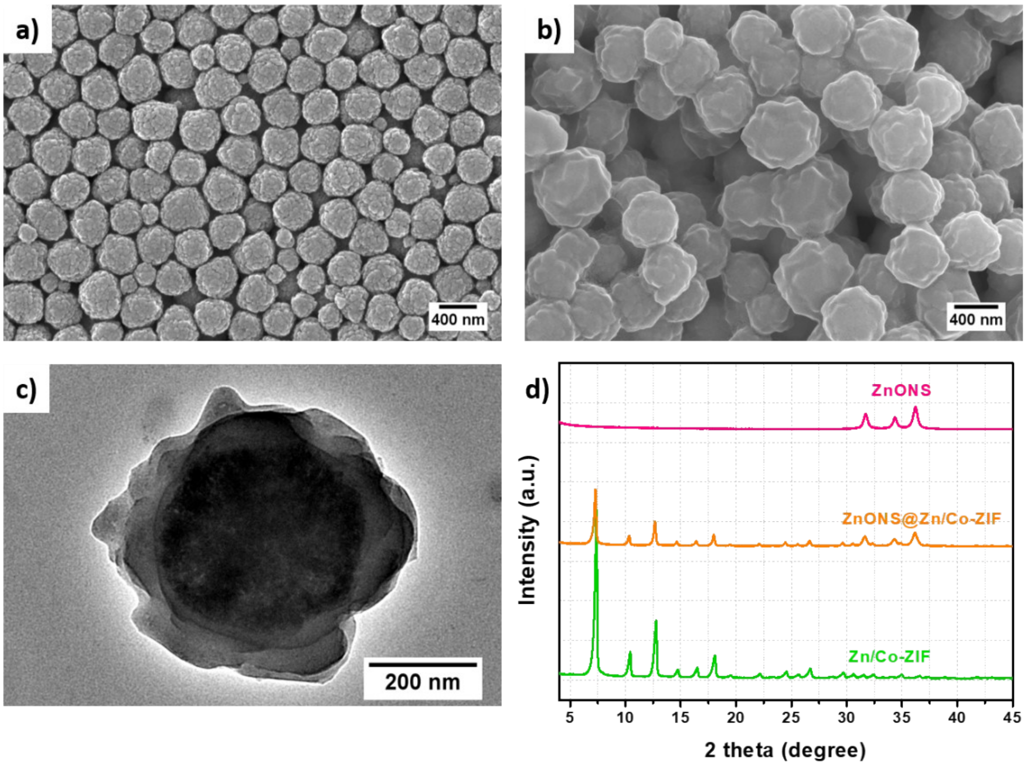

Fig. S1 (a, b) SEM images of ZnO nanosphere (ZnONS) and ZnO@Zn/Co-ZIF. (c) TEM image of ZnO@Zn/Co-ZIF. (d) XRD patterns of Zn/Co-ZIF, ZnONS@Zn/Co-ZIF and ZnONS.

Figure S1 shows the SEM images of ZnO templates and ZnO@Zn/Co-ZIF composites. The TEM image and XRD pattern of ZnO@Zn/Co-ZIF confirmed the core−shell structure.

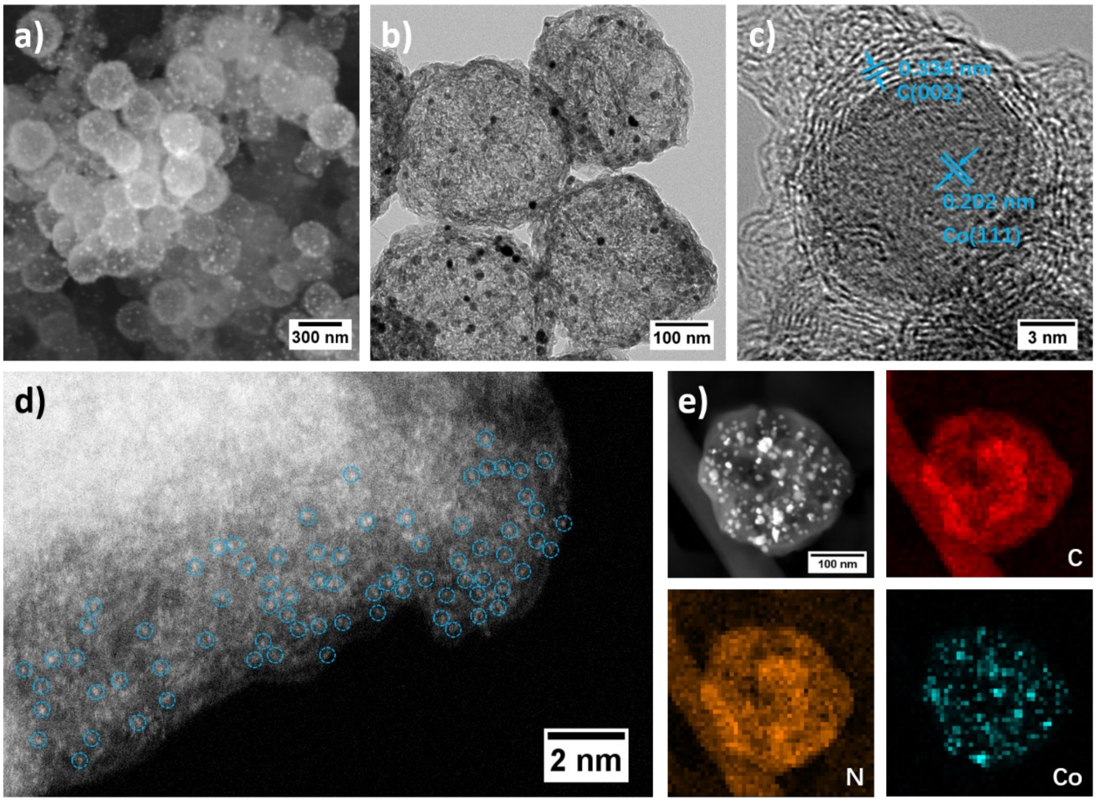

Fig. S2 (a) SEM, (b) TEM and (c) high-resolution TEM images of CoNP/CoN$_x$/CNB, (d) SubÅngström-resolution HAADF-STEM image of CoNP/CoN$_x$/CNB, isolated cobalt atoms are highlighted with blue circles for better observation. (e) HAADF-STEM image and analogous element maps of CoNP/CoN$_x$/CNB.

Fig. S2a and S2b shows the SEM and TEM images of CoNP/CoN$_x$/CNB. The CoNP/CoN$_x$/CNB have diameters of around 400 nm and shell thickness of around 10 nm. Fig. S2c shows that the Co nanoparticles with diameter of around 8 nm are uniformly distributed in the carbon shell and encapsulated by few-layer graphene. The Sub-Ångström-resolution HAADF-STEM image in Fig. S2d shows the presence of isolated Co atoms (highlighted in circles). Fig. S2e shows the STEM image of CoNP/CoN$_x$/CNB and the corresponding element mapping (C, N, and Co).

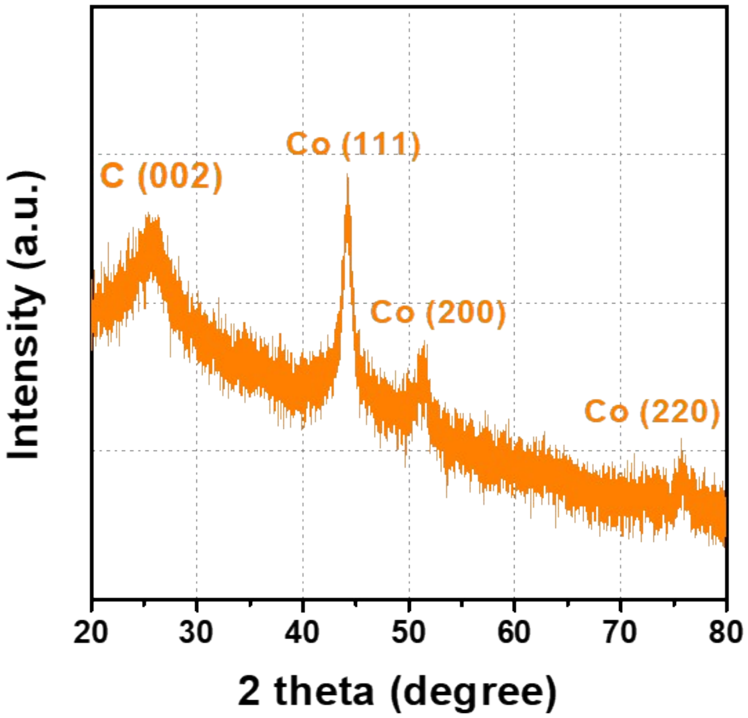

Fig. S3 XRD pattern of CoNP/CoN_x/CNB.

Fig. S3 shows a broad diffraction peak at 26°, corresponding to the (002) plane of graphitic carbon. The remaining peaks at 44.2, 51.5, and 71.3° were ascribed to the (111), (200), and (220) diffractions of face-centered Co^0, respectively.

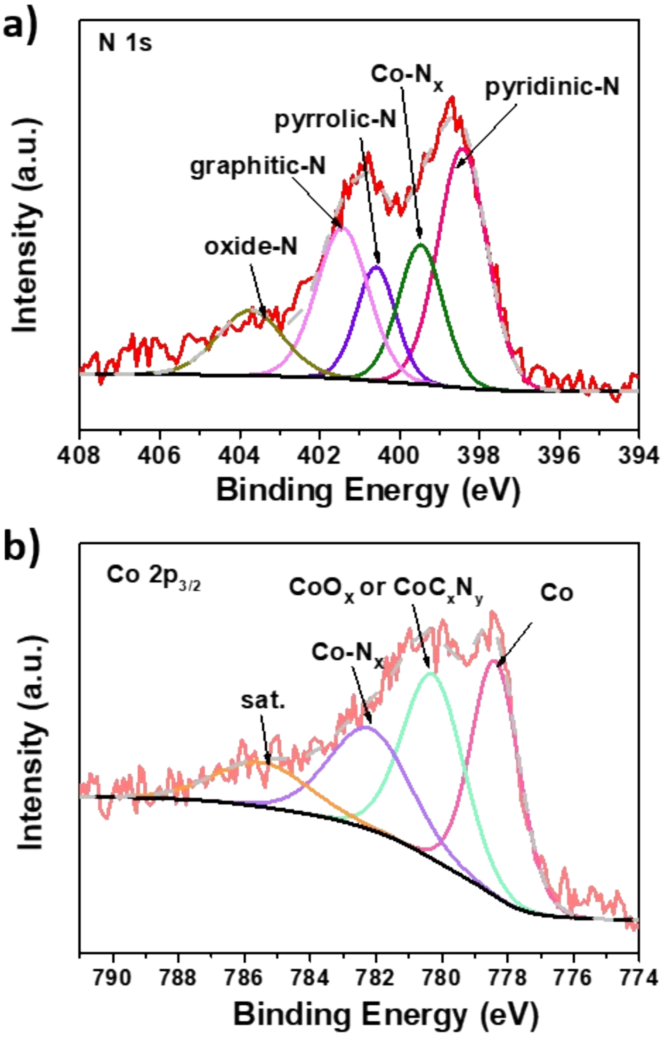

Fig. S4 (a) High-resolution deconvoluted N 1s and (b) Co 2p$_{3/2}$ XPS spectrum of CoNP/CoN$_x$/CNB.

Fig. S4a shows the deconvoluted N 1s spectrum, which verifies the presence of Co−N$_x$ species, as well as the presence of pyridinic-N, pyrrolic-N, graphitic-N, and oxide-N. The deconvoluted Co 2p spectrum shows three peaks located at ~778.4, 780.3, and 782.2 eV, which are associated with Co^0, CoO$_x$, and Co−N$_x$ species, respectively (Fig. S4b).

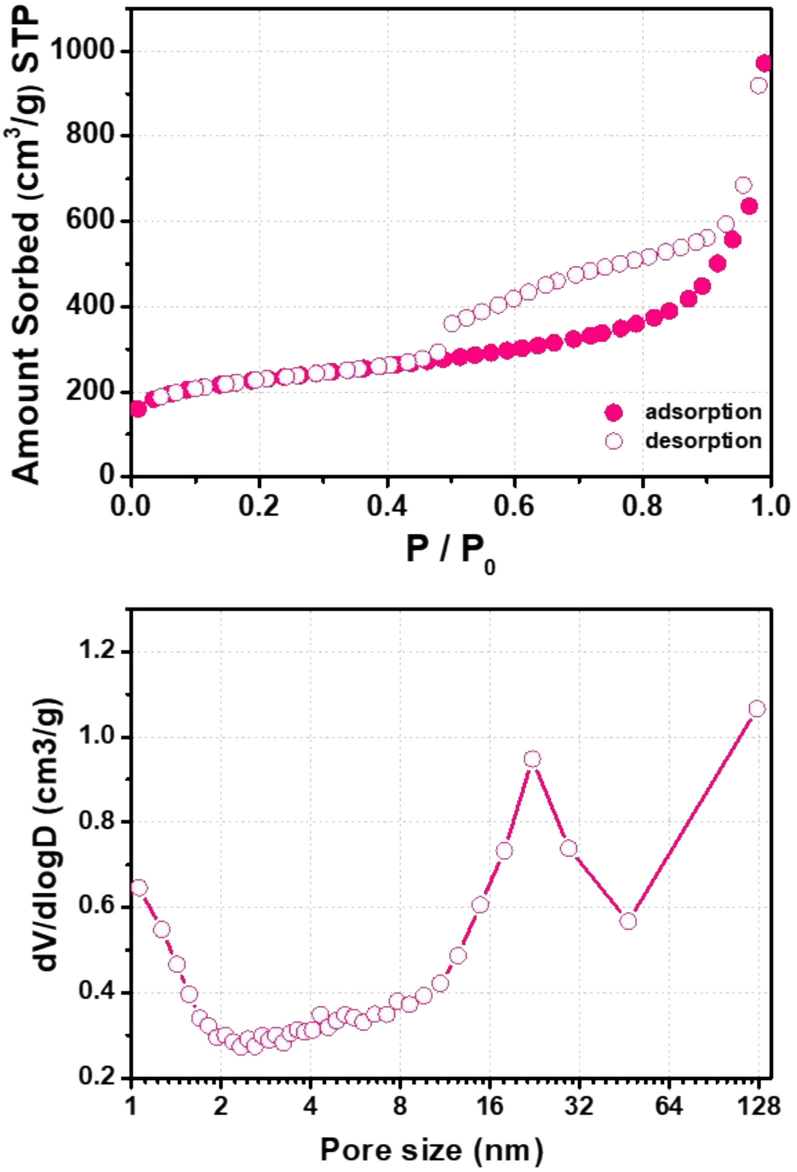

Fig. S5 (a) N_2 sorption isotherm of CoNP/CoN_x/CNB at 77 K, and (b) Pore size distribution of CoNP/CoN_x/CNB.

The porous texture of CoNP/CoN_x/CNB was characterized by N_2 sorption at 77 K (Fig. S5a). The measured Brunauer−Emmett−Teller (BET) surface area is as high as 753 m^2 g^{-1}. The pore size distribution calculated from the desorption branch was shown in Fig. S5b. The continuous pore size distribution indicates that the CoNP/CoN_x/CNB has a hierarchically porous structure.

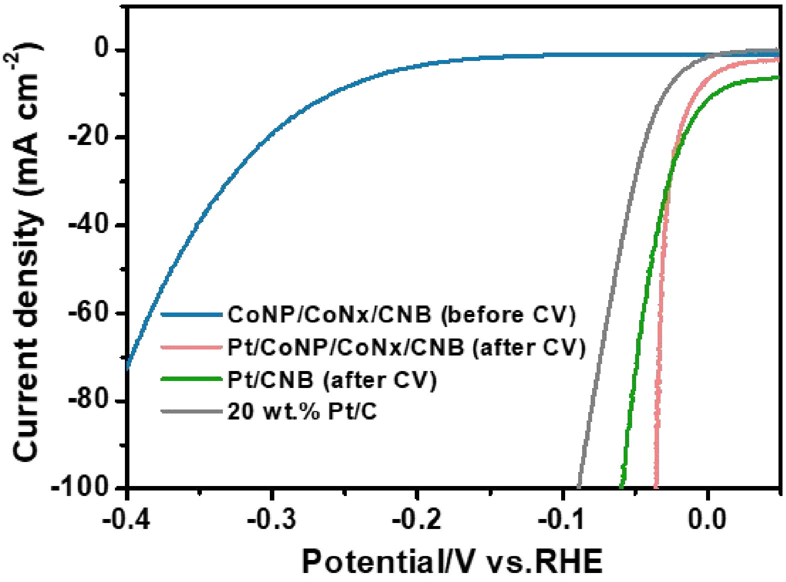

Fig. S6 HER polarization curves of 20 wt.% Pt/C, CoNP/CoN$_x$/CNB, Pt/CoNP/CoN$_x$/CNB and Pt/CNB.

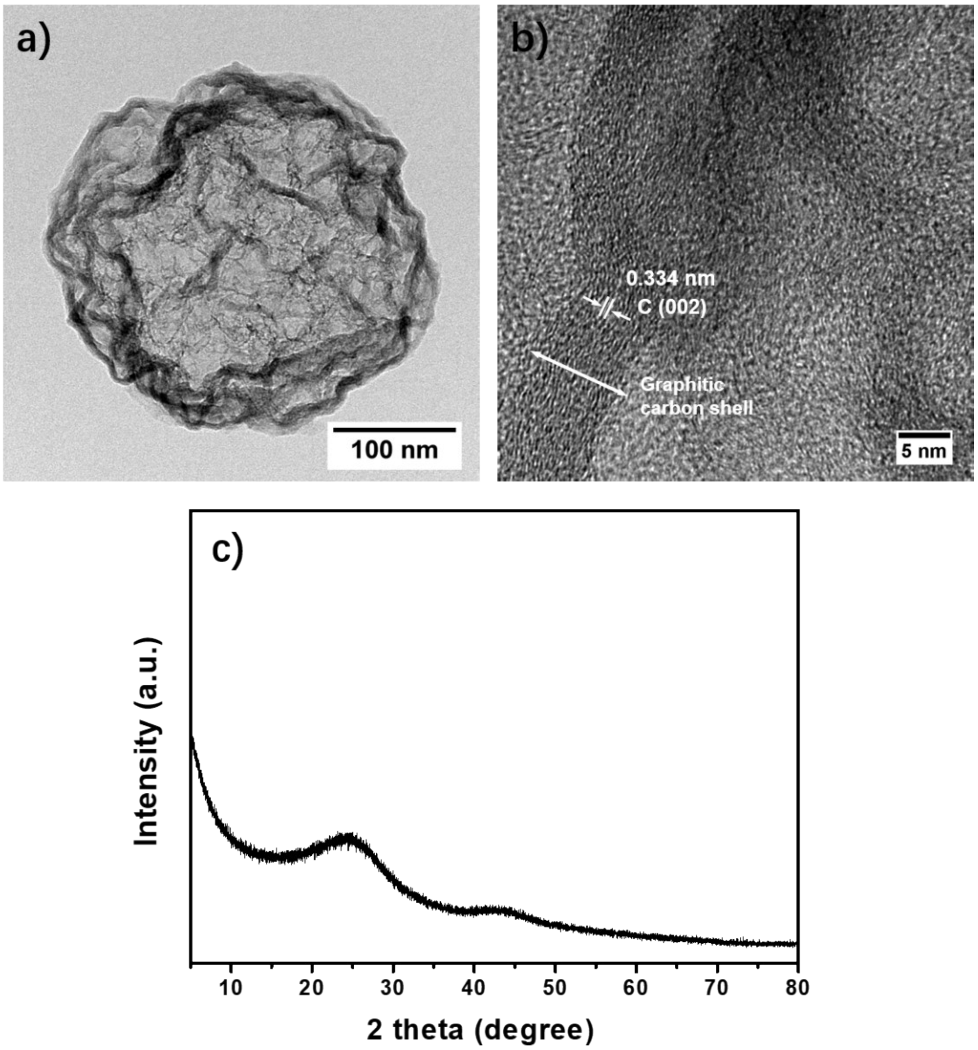

Fig. S7 (a) TEM (b) HR-TEM images and (c) XRD pattern of CNB.

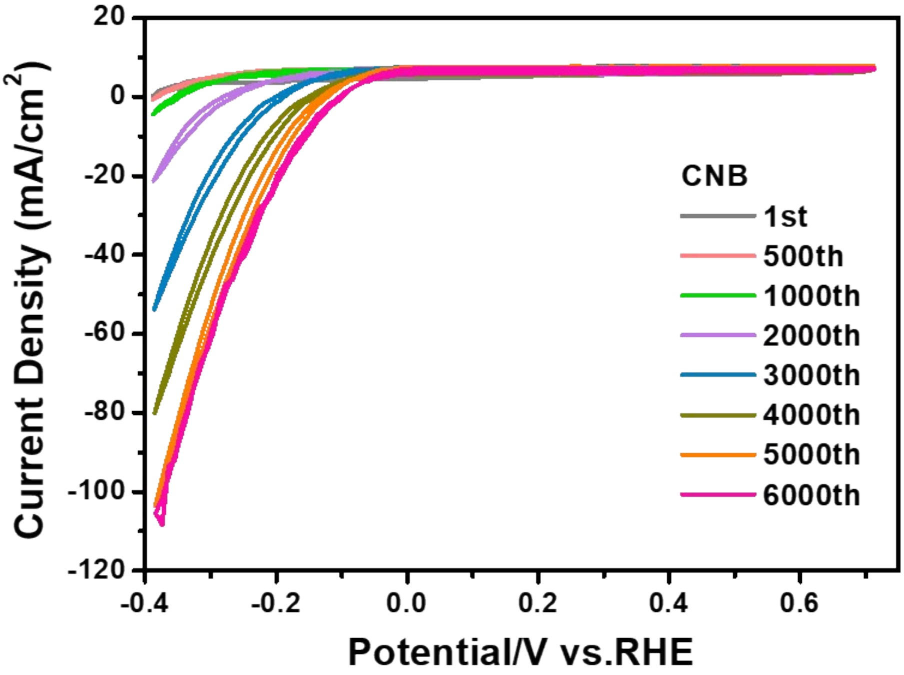

Fig. S8 Representative CVs of CNB in N_2 saturated 0.5 M H_2SO_4 from the 1^{st} to 6000^{th} cycle.

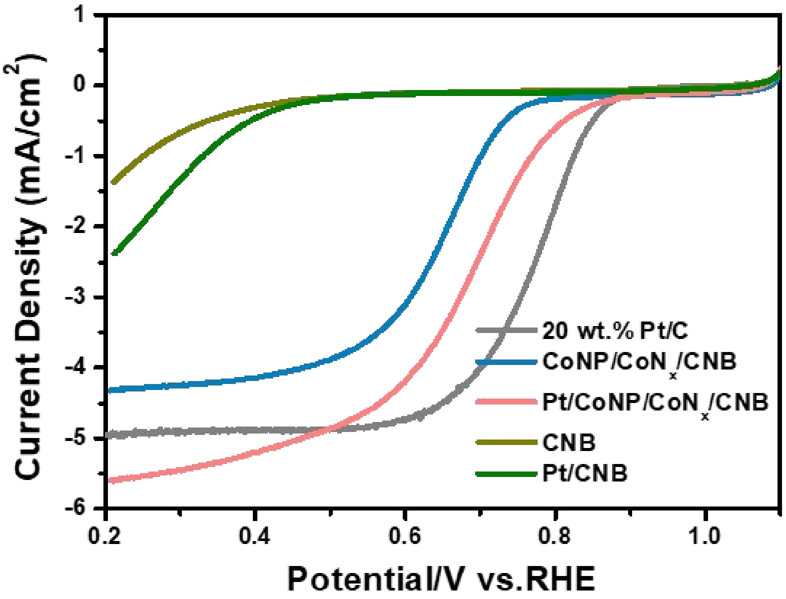

Fig. S9 ORR polarization curves of 20 wt.% Pt/C, CoNP/CoN$_x$/CNB, Pt/CoNP/CoN$_x$/CNB, CNB and Pt/CNB.

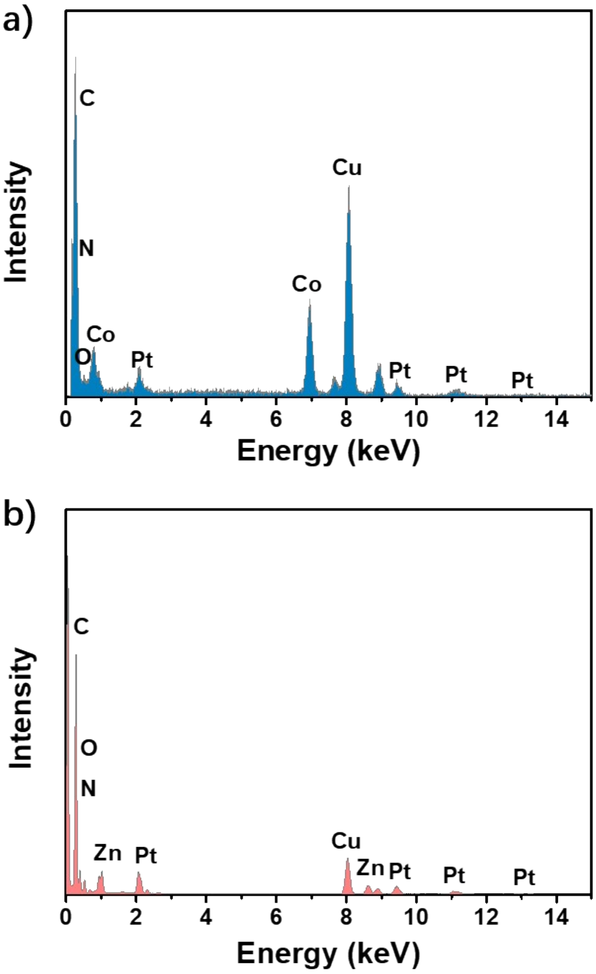

Element	wt%	at %
C K	64.07	83.42
O K	3.55	3.47
N K	9.13	7.52
Co K	20.15	5.35
Pt M	3.10	0.25
Total	100.00	100.00

Element	Wt%	at %
C K	74.76	88.40
N K	6.62	6.71
O K	3.68	3.27
Zn K	3.68	0.80
Pt M	11.26	0.82
Total	100.00	100.00

Fig. S10 EDS analysis of (a) Pt/CoNP/CoN$_x$/CNB and (b) Pt/CNB.

Table S1. Element content (wt%) of Pt/CoNP/CoN_x/CNB and Pt/CNB measured by EDS.

Sample	**Pt/CoNP/CoN_x/CNB (EDS)**	**Pt/CNB (EDS)**
C	64.07%	88.40%
N	9.13%	6.62%
O	3.55%	3.68%
Co	20.15%	-
Pt	3.10%	11.26%

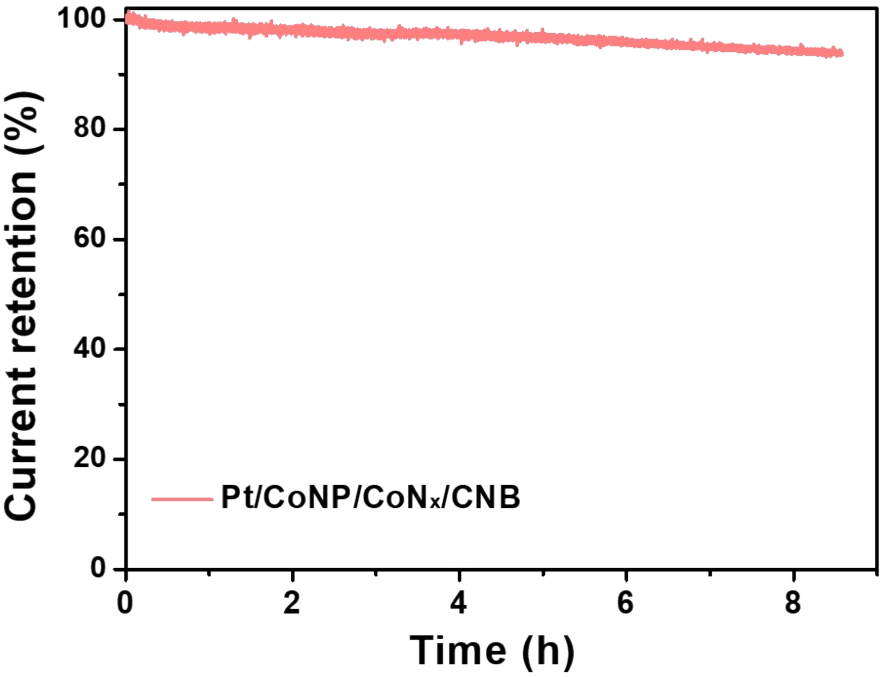

Fig. S11 ORR chronoamperometric curve of Pt/CoNP/CoN_x/CNB.

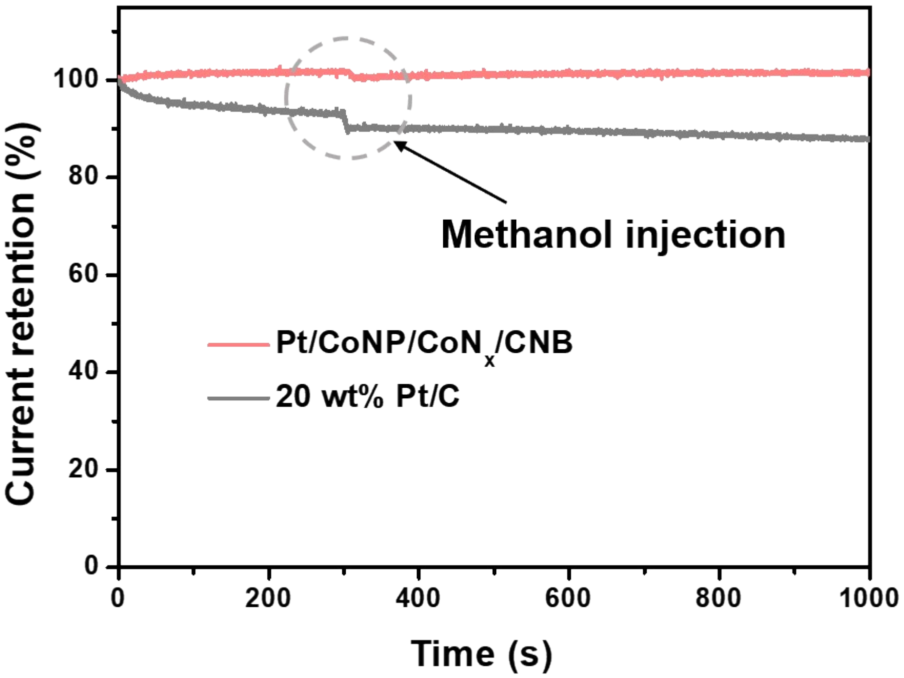

Fig. S12 The chronoamperometric responses with the injection of 3 M methanol.

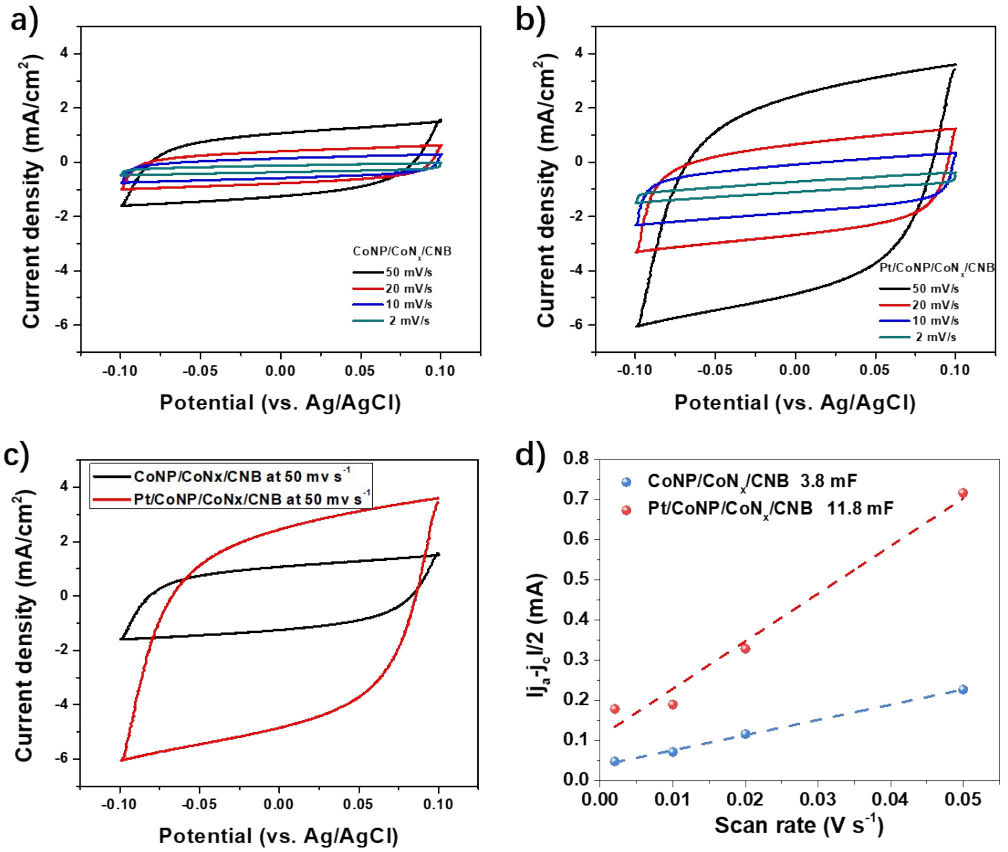

Fig. S13 CV curves at different potential scan rates from 2 to 50 mV s^{-1} for (a) CoNP/CoN$_x$/CNB and (b) Pt/CoNP/CoN$_x$/CNB. (c) CV curves at a scan rate of 50 mV s^{-1} for CoNP/CoN$_x$/CNB and Pt/CoNP/CoN$_x$/CNB. (d) The double layer capacitance (C_{dl}) plots obtained from CV curves.

The electrochemically active surface area (ECSA) calculation was based on the equation:

$$ECSA = \frac{C_{dl}}{C_s}$$

$$C_s = 0.035 \text{ mF cm}^{-2}$$

Table S2. Comparison of ORR performance of the electrocatalysts reported recently with Pt/CoNP/CoN$_x$/CNB in acidic media.

Smaple	**electrolyte**	**Half-wave potential (V vs. RHE)**	**Reference**
Pt/CoNP/CoN$_x$/CNB	0.5 M H_2SO_4	0.68	this work
Co_9S_8/NVC-G	0.5 M H_2SO_4	0.60	*ChemElectroChem*, 2020, 7, 3123.
Fe-PCNRs-700	0.5 M H_2SO_4	0.71	*J. Alloys Compd.*, 2021, 868, 159015.
FeSMCSt5	0.5 M H_2SO_4	0.61	*ACS Appl. Mater. Interfaces*, 2021, 13, 42693.
Co-VN-NC-800	0.5 M H_2SO_4	0.70	*ACS Sustainable Chem. Eng.*, 2020, 8, 8, 3291.
FeSA/AC	0.1 M $HClO_4$	0.68	Nano Energy, 2021, 80, 105534.
Fe_{NP}–N–C	0.1 M $HClO_4$	0.67	*Nat. Commun.*, 2020, 11, 2831.
Co@COF_{900}	0.1 M $HClO_4$	0.65	*Small*, 2019, 1905363.